

Predicting the In-Service Performance of Materials Exposed to Outdoor Weathering

Christopher White, Dr., National Institute of Standards and Technology, Gaithersburg, MD

Kar Tean Tan, Dr., National Institute of Standards and Technology, Gaithersburg, MD

Donald Hunston, Dr., National Institute of Standards and Technology, Gaithersburg, MD

1. Introduction

Sealants are filled elastomers and are an essential component of modern construction, particularly for high-rise structures having curtainwalls. They provide weatherproofing for structures by preventing unwanted water intrusion in the joints between similar and different materials. Sealants are exposed to various aging factors, including temperature, humidity, ultraviolet (UV) radiation, cyclic fatigue deformation, airborne chemicals, and abrasion, all of which inevitably affect the long-term durability of sealants [1-4]. Over the past two decades, rapid technological advances and tremendous market growth in the sealant industry have given rise to a multitude of novel sealant products. Unlike sealants that have been in use for many years and have a proven track record based on outdoor weathering as a standard for performance, these novel products suffer from the lack of effective long-term performance data. Hence, to decrease the risk of introducing poorly-performing sealants into the marketplace, anticipated service lifetimes need to be determined from reliable accelerated laboratory tests.

Various quantification tests have been used to predict long-term performance of sealants more quickly than outdoor field exposures [2, 4]. However, sealants have been reported to fail prematurely in the field even though they have performed satisfactorily in accelerated laboratory tests. Studies by the construction industry indeed have shown a 50 % failure rate within 10 years and a 95 % failure rate within 20 years after installation [5-7]. What makes these failures particularly detrimental is that sealants are often used in areas where moisture-induced degradation is difficult to monitor and expensive to repair. Consequently, sealant failure is frequently detected only after considerable damage has occurred to a structure. In residential housing, premature failure of sealants and subsequent damage by moisture intrusion are a major contributor to the \$65 to \$80 billion spent annually on home repair [8]. The aim of this research was to design laboratory equipment and instrumentation to accelerate degradation of sealants and develop systematic methods for screening the relative importance of four different aging factors that affect sealant degradation: temperature, relative humidity, UV radiation, and cyclic fatigue

deformation. The results from laboratory tests are correlated with outdoor field exposure because field exposure is still a critical component for determining standards of performance.

2. Experimental

2.1 Materials and specimen preparation

Two commercial sealants provided by members of a National Institute Standards and Technology/industry consortium were fabricated into sealant joints conforming to geometry in ASTM C719 (Figure 1) [9]. The exact chemistry of these sealants was unknown so they will be simply denoted as Sealants A and C.

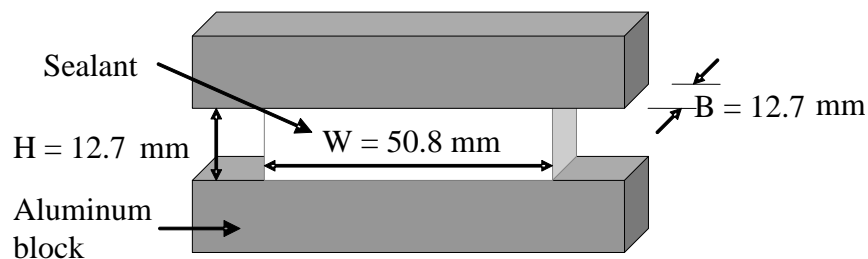


Figure 1. Schematic illustration of the test geometry used (not to scale).

2.2 Laboratory exposure conditions and characterization

Four custom-built sealant testing chambers employed in this study have the ability to independently control temperature (± 0.2 °C), relative humidity (RH) ($\pm 0.5\%$), UV radiation, and deformation. Since the deformation can be controlled, mechanical characterization tests can be performed without removing the specimens from the chamber. A full description of the chamber design is documented elsewhere [10]. Control of temperature was achieved via a precision temperature regulator; humidity control was accomplished by proportional mixing of dry and saturated air; while a highly uniform flux of UV radiation was attained by attaching the chambers to an integrating sphere-based radiation source (Simulated Photodegradation via High Energy Radiant Exposure (SPHERE)) [11]. The SPHERE produces a collimated highly-uniform UV flux of approximately 500 W/m^2 in the wavelength range from 295 nm to 400 nm. The sealant specimen is attached between a fixed grip and a movable grip with a computer-controlled stepper motor and transmission system providing precise movement control. Each chamber has two motors with four specimen holders on each motor for a total of eight specimen holders. Each specimen holder was attached to a hermetically sealed load cell with a capacity of $\pm 113.4 \text{ kg}$. Two

linear variable differential transformers (LVDT), one for each motor, with a deflection range of ± 6.35 mm were used to measure sealant movement. Data from load cells and LVDTs were fed directly to a Keithley 2701 Ethernet-based data acquisition system. A custom-written LabVIEW program was used to collect the voltage measurements from the Keithley system every 15 seconds, 24 hours a day. The data was averaged once per minute and appended to a tab-delimited database on a remote server.

Specimens were either subjected to no mechanical deformation (denoted as ‘static’) or cyclic fatigue deformation (denoted as ‘cyclic’). In cyclic fatigue tests, a total of 1460 cycles was imposed on each specimen over the course of a month (38 min/cycle) using a triangle wave varying from 0 % to 25 % strain. Prior to and after the exposure tests, the mechanical properties of the specimens were characterized using a specific protocol. The sample was first subjected to two loading-unloading-recovery cycles to a maximum strain of 26 %. The specimens were then subjected to a stress relaxation measurement at a strain of 18 %. The strain history used is shown in Figure 2. The loading-unloading tests utilized a cross-head speed of 2.64 mm/min so the total time under load was 150 s. To allow for viscoelastic recovery, the sample was held at 0 % strain for 1,500 s before the next step. The motivation for the two loading-unloading cycles was to quantify what is known as the Mullins effect and eliminate its influence in the subsequent characterization test. The Mullins effect occurs in many polymers and is characterized by a higher stress being produced at a given strain the first time the specimen is deformed compared to that produced at the same strain in subsequent deformations. As long as the maximum strain achieved during the first deformation is not exceeded, all subsequent loadings follow the same loading curve so results are reproducible. In the stress relaxation test, the cross-head speed was 70 mm/min which meant the specimen reached the hold strain in just under 2 s. To allow for the non-instantaneous loading, data point at less than 15 s were ignored. The load was then monitored for 2.5 h, useful data were obtained between 15 s and 9,000 s. Following the stress relaxation test, a recovery experiment was performed in which the sample strain was taken to 0 % and the stress was monitored for 2.5 h.

From the stress relaxation data, an apparent modulus, E_a , was calculated using a relationship based on the statistical theory of rubber-like elasticity [12-14]:

$$E_a(t, \lambda) = \frac{3L(t)}{WB(\lambda - \lambda^{-2})} \quad (1)$$

where W and B are the width and breath of the sealant (Figure 1), L is the load, t is the time and λ is the extension ratio, which is given by:

$$\lambda = 1 + \frac{\Delta}{H} \quad (2)$$

where Δ is the cross-head displacement and H is the undeformed height of the sealant. A fractional change in apparent modulus, F , was used to characterize the effect of environment on E_a :

$$F = \frac{E_a(t)}{E_{a,0}(t)} \quad (3)$$

where $E_{a,0}(t)$ and $E_a(t)$ are the apparent moduli before exposure and after exposures, respectively.

During cyclic fatigue or static tests, specimens were exposed to one of four environments involving combinations of temperature and RH, i.e., (a) 30 °C and 0 % RH, (b) 30 °C and 75 % RH, (c) 50 °C and 0 % RH, and (d) 50 °C and 75 % RH. Henceforth, 50 °C will be denoted as ‘hot’, and 30 °C as ‘cold’; 75 % RH will be denoted at ‘wet’, and 0 % RH as ‘dry’. The effect of UV radiation on the durability of sealant is currently being investigated, and will be published in the near future.

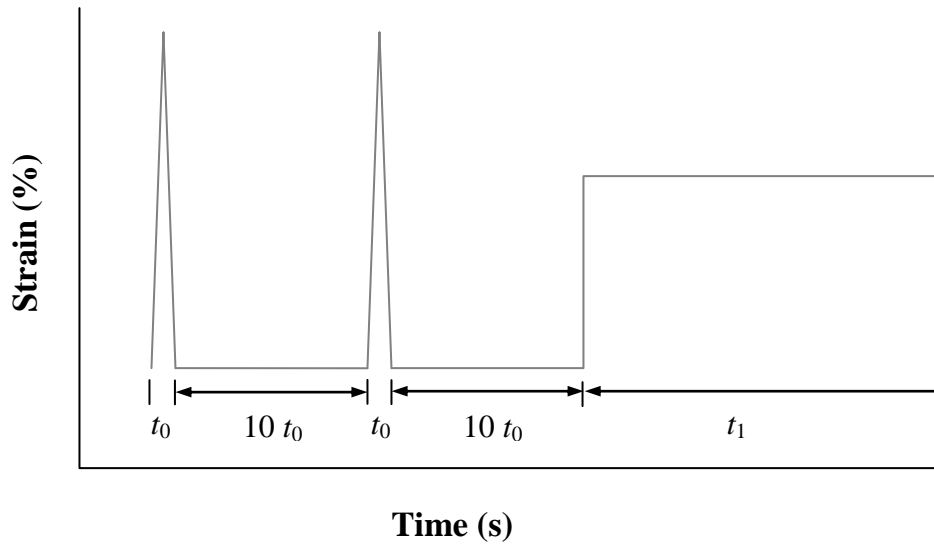


Figure 2. Strain history used for Mullin cycles and stress relaxation tests.

2.3 Field exposure and characterization

Field exposure was performed in Gaithersburg, MD using custom-made thermally-driven outdoor exposure engines, as shown in Figures 3 and 4. Each apparatus was composed of a fixed-support frame and a moving frame. The fixed frame was made from wood and designed so that its length changed very little with the temperature variations during the year. The moving frame consisted of two 101.6 mm diameter polyvinyl chloride (PVC) pipes (Schedule 40) which have a significant thermal expansion coefficient. The two frames are joined at one end and capped with custom stainless steel crosspieces at the other ends. Six sealant specimens are attached between the crosspieces so the thermally driven expansion and contraction of the PVC pipes produce strains in the specimens. The samples are held in place by grips attached to the crosspieces with stainless steel rods. Each grip had a separate load cell to monitor force while the displacement was measured with two LVDTs attached between the crosspieces, one attached at each end. The daily temperature variation produced a cyclic fatigue deformation in the sealant specimens. A full description of the devices is to be found elsewhere [15]. Specimens were placed into the device at a time when the temperature was approximately 13 °C (55 °F) so they were under no load at that temperature. Two different types of engines were used: ‘summer/tension’ (Figure 3) and ‘summer/compression’ engines (Figure 4). For ‘summer/tension’ engines, PVC pipes expanded at high temperatures and caused specimens to load in tension; conversely, specimens were loaded in compression when pipes contracted at low temperatures, as shown schematically in Figures 3b and 3c. With the ‘summer/compression’ design, the apparatus placed specimens in tension during the winter (winter/tension) and in compression during the summer (‘summer/compression’) (Figures 4b and 4c). Each apparatus was placed vertically facing south. For comparison, 2 specimens of each sealant were placed nearby so they received the same exposure but with no applied strains. At approximately six-month intervals, the specimens were removed from the exposure setting and characterized on the same device used for the laboratory experiments. Before testing, external loads were applied to the specimens to force them back to their original, unexposed dimensions. For the sealants studied here, experimental evidence has shown that 10 days were sufficient to do this. The specimens were then characterized using the same two loading-unloading-recovery cycles followed by a stress relaxation measurement. After this, the specimens were returned to outdoor exposure in the same position as before. Consequently, the specimens that were under tension in the summer were subjected to compression in the winter and vice versa.

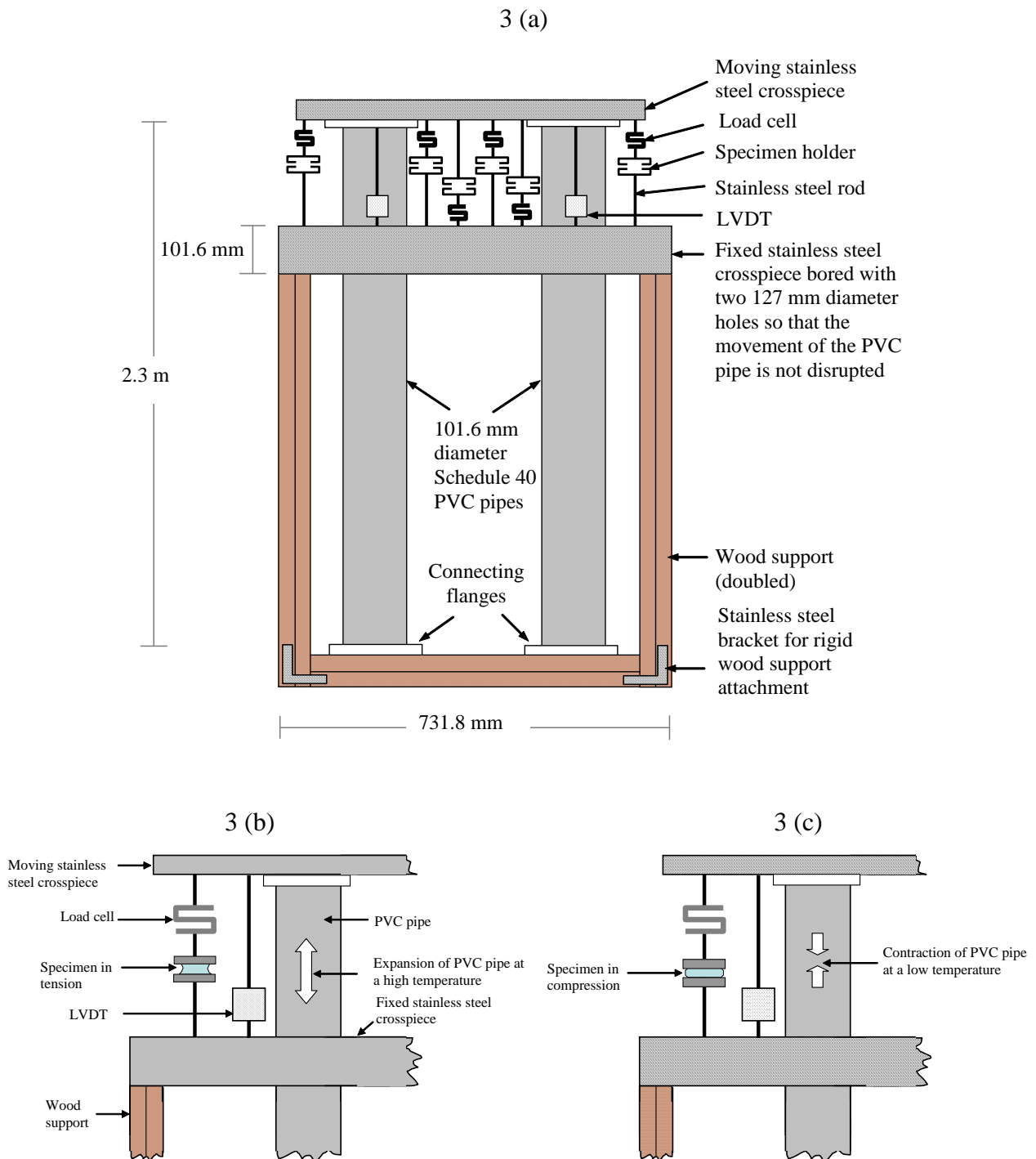


Figure 3. Schematic illustrations of (a) the thermally-driven ‘summer/tension’ PVC engines, and the mechanism of the apparatus: (b) at a high temperature, the PVC pipe expands causing the specimen in tension; and (c) at a low temperature, the pipe contracts causing the specimen in compression.

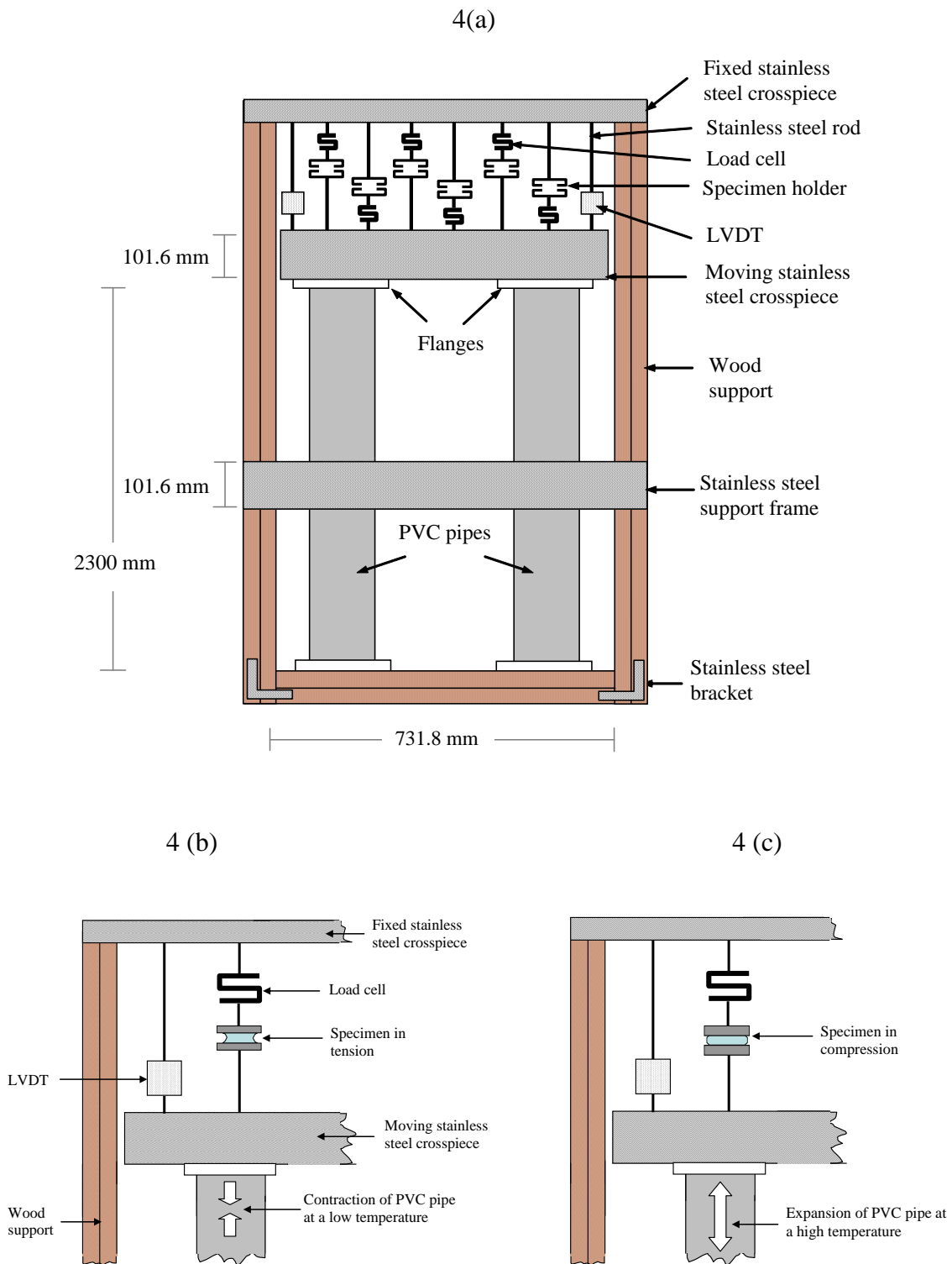


Figure 4. Schematic illustration for the mechanism of the thermally driven ‘summer/compression’ PVC engine (not to scale): (a) at a low temperature, the PVC pipe contracts causing the specimen in tension; and (b) at a high temperature, the pipe expands causing the specimen in compression.

3. Results and Discussion

3.1 Exposure under Laboratory Conditions

Representative apparent moduli vs. relaxation time curves for specimens under ‘cyclic/cold/wet’ conditions prior to exposure and after completion of cyclic fatigue deformation in the NIST SPHERE for one month are shown in Figure 5. There were up to four replicates in each test, and the vertical bars indicate experimental uncertainty. The difference seen in Figure 5 between the two curves is significant. Note that there is no change in the curve shape, implying that time dependence of the apparent modulus is similar before and after exposures. However, the magnitude of apparent modulus decreased by a small amount after exposure. Similar curves can be generated for all eight exposure conditions. To facilitate comparison between different exposure conditions, stress relaxation data are presented as a fractional change in apparent modulus (F), as a function of relaxation time (see Equation 3, Figure 6). In such a graph, no change would be represented as a horizontal straight line at $F=1$. A horizontal line above or below $F=1$ indicates that exposure caused a vertical shift in the stress relaxation curve but no change in shape; i.e., the time dependence of the modulus did not change. Anything other than a horizontal straight line indicates a change in the time dependence. The experimental uncertainty can be shown as a hashed region on each side of $F=1$ so if the points for a given curve fall within this region, there is no change outside the experimental uncertainty.

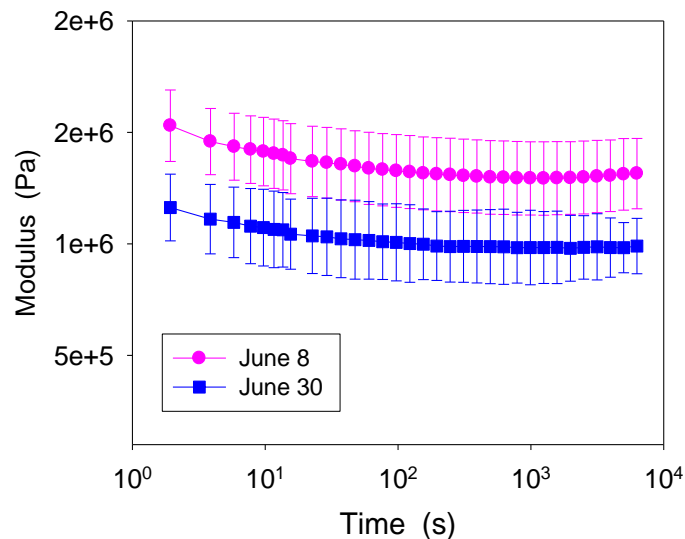


Figure 5. Variation of apparent modulus as a function of relaxation time for Sealant C under ‘cyclic/cold/wet’ conditions before and after exposures.

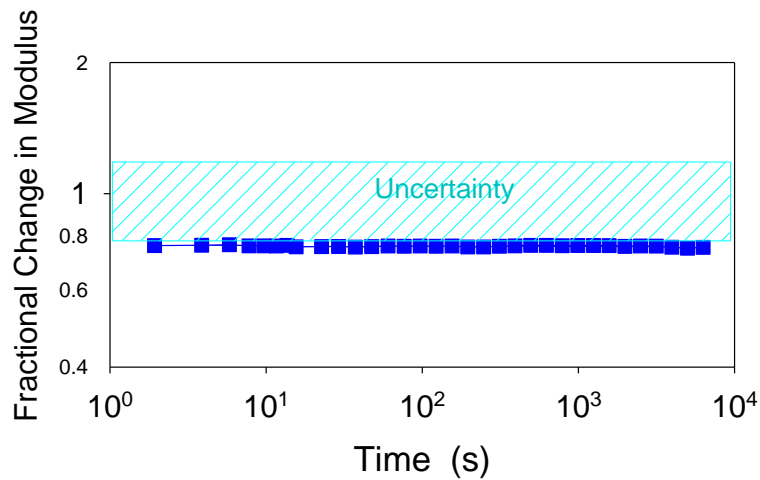


Figure 6. Variation of fractional change in modulus as a function of relaxation time for Sealant C under ‘cyclic/cold/wet’ conditions before and after exposures.

The variations of fractional change in relaxation modulus with time for different combinations of temperature, mechanical movements and RH for Sealant A is shown in Figure 7 after one month in the NIST SPHERE. It can be seen that the major effect of environmental exposure was a small increase in the moduli (vertical shift up). For a few conditions, there was also a slight positive slope indicating that the time dependence decreased slightly. This might suggest a small shift in the glass transition temperature of the sealant, or the increase in modulus may simply reduce the effect of the falloff from the glass to rubber transition. The effect of temperature on modulus was examined by comparing ‘static/cold/dry’ with ‘static/hot/dry’, or ‘static/cold/wet’ with ‘static/hot/wet’. These results revealed that a higher temperature led to a larger increase in modulus; thus temperature effects may impact the durability of this sealant. When the dry and wet tests results were compared, no consistent trend could be identified; however, the results for cyclic fatigue (‘cyclic’ vs. ‘static’) clearly indicated that motion had a significant effect. Figure 7 shows that exposure with cyclic fatigue deformation resulted in higher fractional change in modulus than that for the corresponding ‘static’ conditions.

The fractional change in modulus as a function of relaxation time for Sealant C is shown in Figure 8. Just as with Sealant A, the dominant change was a vertical shift. In this case the shift is down, and the plots are near straight lines parallel to the abscissa. The largest effect was cyclic fatigue which produced a significant drop in modulus in 3 of the 4 conditions. Temperature was also important and produced a decrease in modulus for 2 of the 4 cases. In particular, the fractional change in modulus for

‘cyclic/hot/wet’ was 100 % greater than that of ‘cyclic/cold/wet’. In a relatively dry environment only the tests with cyclic fatigue movement and high temperatures produced a significant change in modulus. The moisture-assisted deterioration in modulus can be viewed by comparing ‘cyclic/hot/wet’ with ‘cyclic/hot/dry’, ‘static/hot/wet’ with ‘static/hot/dry’, or ‘cyclic/cold/wet’ with ‘cyclic/cold/dry’. From this comparison, the moisture effect on modulus decrease was clearly seen from all conditions involving either a high temperature, cyclic fatigue deformation or the combination of both factors. The increase in the latter environment was relatively significant. However, the role of moisture in the static performance at a low temperature was comparatively trivial (c.f. ‘static/cold/dry’ and ‘static/cold/wet’). In a ‘cold’ and ‘dry’ environment, cyclic fatigue deformation had no apparent effect on the performance of sealant specimens (c.f. ‘cyclic/cold/dry’ and ‘static/cold/dry’). When the cyclic fatigue movement was applied with a high temperature, a pronounced decrease in fractional modulus was observed (c.f. ‘cyclic/hot/dry’ and ‘cyclic/hot/wet’ conditions).

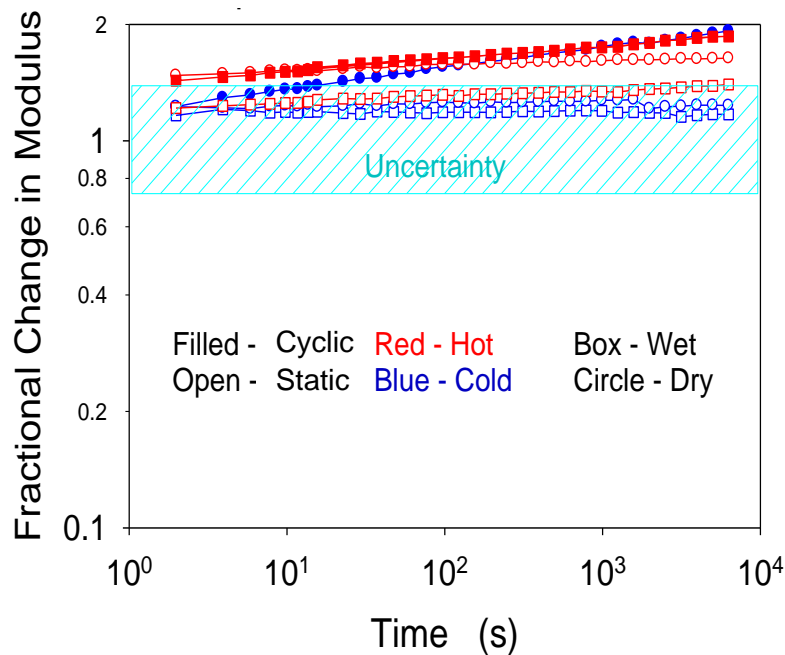


Figure 7. Stress relaxation curve for both static and cyclic fatigue tests of Sealant A.

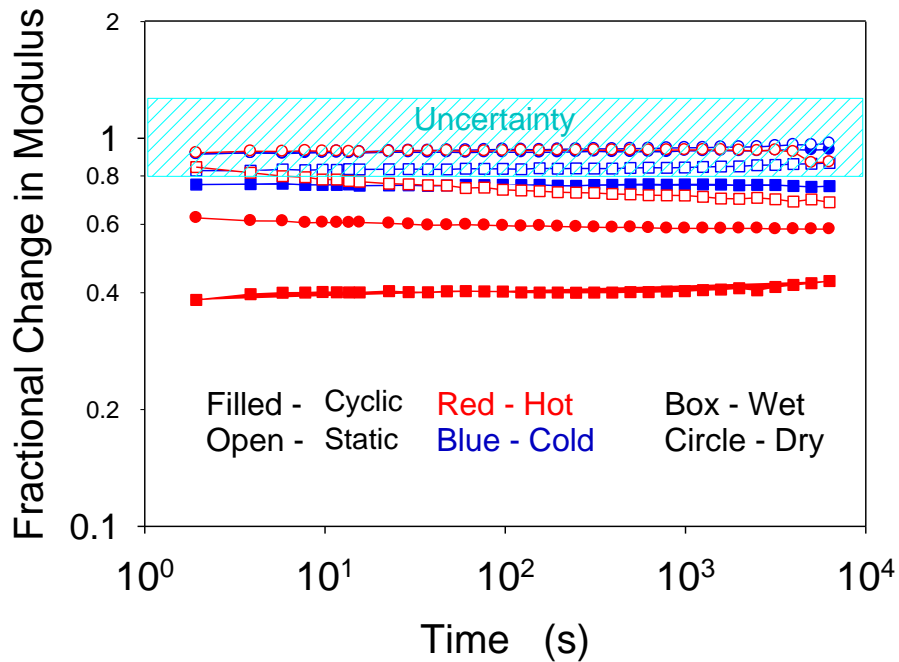


Figure 8. Stress relaxation curve for both static and cyclic fatigue tests of Sealant C.

3.2 Exposure under field conditions

Modulus curves such as those shown in Figure 5 were obtained for each sample before outdoor exposure and at six-month intervals over the two and a half years of exposure. The tests were started in the spring, so the first 6 months are designated ‘summer 1’. Much like the SPHERE data, the major impact of environmental exposure was to shift the curves vertically with little change in shape. Consequently, the analysis can be simplified by focusing on the vertical position of the curves. To characterize the vertical position for each curve, it was decided to determine the value of apparent modulus at 100 s. Figures 9 and 10 show the 100 s moduli values for specimens exposed outdoors with no imposed strain (baseline), strain imposed by the summer tension apparatus, and strain imposed by the ‘summer/compression’ apparatus. In the outdoor testing, it is easy to examine the effect of cyclic fatigue deformation by comparing the baseline data (exposure but no strain) with the cyclic data from the ‘summer/tension’ and ‘summer/compression’ engines. For Sealant A, the baseline data showed a significant increase in apparent modulus after the first summer of outdoor exposure. In subsequent exposure, the apparent modulus for the baseline specimens remained constant or increased slightly over the next two years. This suggests that the exposure, particularly the high temperatures during the first summer, produced either chemical reactions that increased the effective cross-link density or a loss of

solvent which increased stiffness. After the first 6 months, these changes stopped or slowed significantly. This result correlated well with the earlier observations seen for the laboratory accelerated exposure. For those specimens that experienced cyclic strain, the apparent moduli were well below that for the baseline samples with similar exposure. Thus, cyclic fatigue deformation decreased modulus while exposure increased it. This would indicate that two different mechanisms were present at the same time. The results in Figure 9 also indicate that tension had a larger effect than compression. In all but one case, tension produced a larger change relative to the baseline than compression regardless of temperature. Overall, however, the changes after 2.5 years of exposure were smaller than those observed in the laboratory tests. Unlike the outdoor exposure, modulus changes were readily detectable after a month of exposure under relatively more severe laboratory test conditions. Although the outdoor results gathered thus far show only small changes, these preliminary results showed potential for establishing correlations between the outdoor and indoor accelerated tests. The monitoring of modulus change in outdoor specimens is continuing.

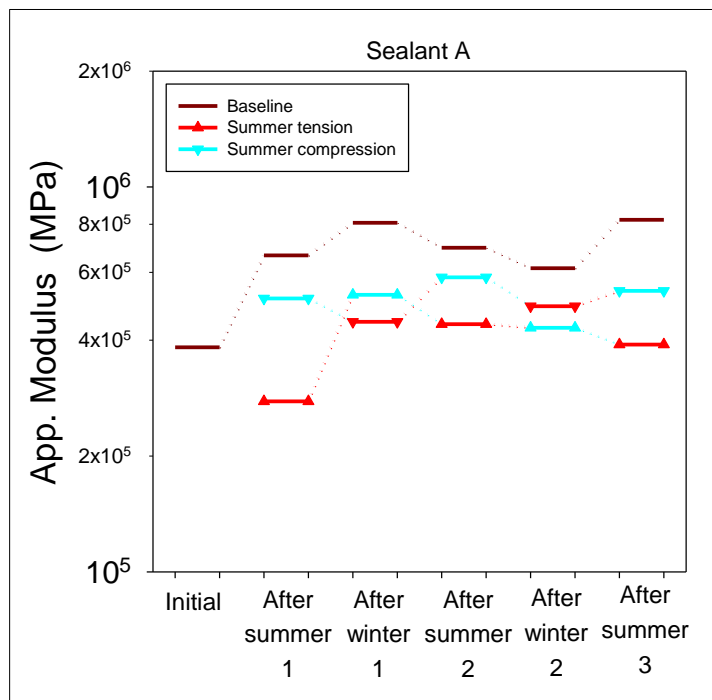


Figure 9. Modulus change as a function of time for Sealant A exposed to outdoor weathering.

The apparent modulus changes as a function of exposure for Sealant C is shown in Figure 10. Unlike Sealant A, the modulus of outdoor exposed Sealant C without any mechanical strain (baseline) did not undergo any changes even after 2.5 years of exposure. Under temperature-driven cyclic fatigue loading,

a decrease in modulus was observed after the first summer for both ‘summer/tension’ and ‘summer/compression’ engines. A greater modulus decrease was seen for the ‘summer/tension’ engines. The initial modulus decrease in Sealant C after the first summer was also seen for Sealant A (see Figure 9). In subsequent exposure with cyclic strain, there was some recovery of modulus, but the values were always below those from the baseline tests. This observation agreed with that seen from the laboratory accelerated exposures. Similar results have been reported in the literature. In the study of various latex and solvent-borne acrylic sealant products, Karpati [16] also found that cyclic fatigue movement was the major aging factor during outdoor exposure and that outdoor weathering alone had a negligible effect. As with Sealant A, Figure 10 shows that tension had a larger effect than compression or temperature, since the largest modulus decrease in each set of tests was in the specimens in tension. The laboratory tests utilized only tension, so a comparison with compression results is not possible. Temperature, however, seems to be more important in the laboratory tests than the outdoor results so far. There are two reasons for this. First, the outdoor specimens saw both hot and cold temperatures during exposure, and second, the temperature range studies in the laboratory extended to much higher values, which would greatly accelerate any effects. More time is needed in the outdoor tests to establish and test a correlation.

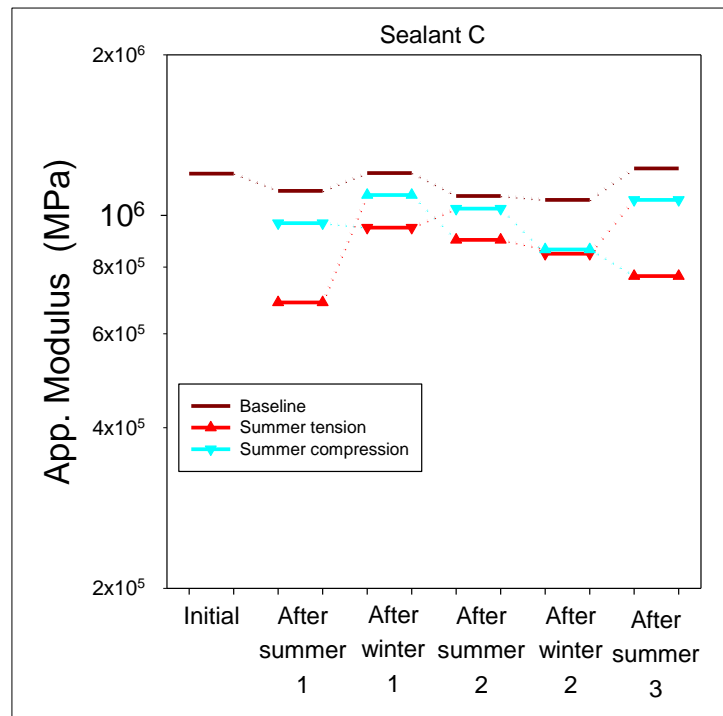


Figure 10. Modulus change as a function of time for Sealant C exposed to outdoor weathering.

4. Conclusions

Test methods were developed to duplicate the failure modes that occur in sealants during environmental exposure. The methods used a systematic approach to identify independent and synergistic effects of various aging factors on the durability of sealants. Two different types of sealants were studied, which were denoted as Sealants A and C. Sealants were evaluated for changes in modulus and stress relaxation. Changes in modulus were monitored over time in accelerated laboratory exposure over one month period while field exposure was evaluated every six months. Laboratory tests revealed that high temperature and cyclic fatigue deformation had a significant effect in increasing the modulus of Sealant A. For Sealant C, laboratory exposure showed that, in the absence of cyclic fatigue deformation, only the combination of high temperature and humidity produced a significant decrease in modulus. With cyclic fatigue deformation, only the specimens tested in cold, dry conditions failed to show a decrease in modulus. The preliminary outdoor exposure results for Sealant A showed promising correlation in that a modulus increase was observed for outdoor exposed specimens without any cyclic fatigue deformation and for laboratory-accelerated specimens. In the case of Sealant C, sealants exposed to field conditions exhibited little change without cyclic fatigue deformation, which agrees with the results from the accelerated laboratory test. Consequently, although the results are still preliminary, the methodology shows promise as a means to estimate service life of sealants in field conditions similar to those the sealant may encounter under actual use conditions. The present study has clearly showed the importance of designing experiments that enable the various aging factors to be systematically evaluated.

5. Literature citations

1. Tan KT, White CC, Benatti DJ, Stanley D and Hunston DL, Chemorheological investigation on the environmental susceptibility of sealant, in: *Handbook of Sealant Technology*, Mittal KL and Pizzi A (Eds.), CRC Press, New York, pp. 75-92 (2009).
2. Wolf AT, Ageing resistance of building and construction sealants, in: *Durability of Building Sealants*, Beech JC and Wolf AT (Eds.), E & FN Spon, London, UK pp. 63-89 (1996).
3. Lacher S, Williams RS, Halpin C and White CC, Development of a powered outdoor sealant fatigue test apparatus, in: *Service Life Prediction: Challenging the Status Quo*, Martin JW, Ryntz RA and Dickie RA (Eds.), Federation of Societies for Coatings Technology, Bluebell, PA, pp. 207-216 (2005).
4. Searle ND, Natural and artificial weathering of sealants, in: *Handbook of Sealant Technology*,

Mittal KL and Pizzi A (Eds.), CRC Press, New York, pp. 93-142 (2009).

5. Woolman R and Hutchinson A, *Resealing of Buildings: A Guide to Good Practice*, Butterworth-Heinemann, Oxford, UK (1994).
6. Grunau E, Service Life of Sealants in Building Construction (in German), Research Report, Federal Ministry for Regional Planning, Building and Urban Planning, Bonn, Germany (1976).
7. Chiba R, Wakimoto H, Kadono F, Koji H, Karimori M, Hirano E, Amaya T, Sasatani D and Hosokawa K, Improvement System of Waterproofing by Sealants in Japan, pp. 175-199, Japan Sealant Industry Association, Tokyo, Japan (1992).
8. Expenditures for Residential Improvements and Repairs – 1st Quarter, Current Construction Reports, US Census Bureau, Department of Commerce, Washington, DC (2002).
9. ASTM C719-93 (2005), Standard test method for adhesion and cohesion of elastomeric joint sealants under cyclic movement (Hockman Cycle), American Society for Testing and Materials, Philadelphia, 1993.
10. White CC, Tan KT, Hunston DL, Hettenhouser J, and Garver JD, A hybrid in-situ accelerated testing device for building joint sealants, in: *Service Life Prediction for Sealants Phase II Report: Precision Exposure Chambers and Screening Experiments*, White CC (Ed.), pp. 10-37, NIST, MD (2007).
11. Chin JW, Byrd E, Embree N, Garver J, Dickens B, Finn T and Martin J, Accelerated UV weathering device based on integrating sphere technology, *Rev. Sci. Instrum.*, 75 (11), 4951 (2004).
12. Taylor CR, Greco R, Kramer O and Ferry JD, Nonlinear stress relaxation of polyisobutylene in simple extension, *J. Rheol.*, 20, 141-152 (1976).
13. Ferry JD, *Viscoelastic Properties of Polymers*, John Wiley & Sons, Inc. 3rd edition, New York (1980).
14. Ketcham SA, Niemiec JM and McKenna GB, Extension and compression of elastomeric butt joint seals, *J. Eng. Mech.*, 122, 669-677 (1996).
15. White CC, Tan KT, O'Brien EP, Hunston DL and Williams RS, Design, fabrication and implementation of thermally-driven outdoor testing devices for building joint sealants, in: *Service Life Prediction for Sealants Phase II Report: Precision Exposure Chambers and Screening Experiments*, C.C. White (Ed.), pp. 38-72, NIST, MD (2007).
16. Karpati KK, Weathering of silicone sealant in strain-cycling exposure rack, *Adhesive Age*, 23, 41-47 (1980)

6. Acknowledgements

The authors thank Dr. Joannie Chin of NIST for insightful discussions. The support from a NIST/industry consortium on Service Life Prediction of Sealant Materials is greatly appreciated. Participating companies include DAP, Degussa, Dow Corning, Kaneka Texas, SIKA, Solvay, Tremco and Wacker Silicones.